NREL
NATIONAL RENEWABLE ENERGY LABORATORY

A Detailed Performance Model for Photovoltaic Systems

Preprint

Hongmei Tian
University of Colorado – Denver and Shenzhen Polytechnic

Fernando Mancilla-David, Kevin Ellis, and Peter Jenkins
University of Colorado – Denver

Eduard Muljadi
National Renewable Energy Laboratory

To be published in the Solar Energy Journal

Journal Article
NREL/JA-5500-54601
July 2012

Contract No. DE-AC36-08GO28308

Available electronically at http://www.osti.gov/bridge

Available for a processing fee to U.S. Department of Energy
and its contractors, in paper, from:

U.S. Department of Energy
Office of Scientific and Technical Information
P.O. Box 62
Oak Ridge, TN 37831-0062
phone: 865.576.8401
fax: 865.576.5728
email: mailto:reports@adonis.osti.gov

Available for sale to the public, in paper, from:

U.S. Department of Commerce
National Technical Information Service
5285 Port Royal Road
Springfield, VA 22161
phone: 800.553.6847
fax: 703.605.6900
email: orders@ntis.fedworld.gov
online ordering: http://www.ntis.gov/help/ordermethods.aspx

Cover Photos: (left to right) PIX 16416, PIX 17423, PIX 16560, PIX 17613, PIX 17436, PIX 17721

Printed on paper containing at least 50% wastepaper, including 10% post consumer waste.

A Detailed Performance Model for Photovoltaic Systems

Hongmei Tian[a,b], Fernando Mancilla–David[☆a], Kevin Ellis[d], Eduard Muljadi[c], Peter Jenkins[d]

[a]*Department of Electrical Engineering, University of Colorado Denver, 1200 Larimer St., Denver, Colorado, 80217 USA*
[b]*Industrial Training Center, Shenzhen Polytechnic, Xili Lake, Shenzhen, Guangdong, 518055 China*
[c]*National Renewable Energy Laboratory, 1617 Cole BLVD, Golden, Colorado, 80401, USA*
[d]*Mechanical Engineering Department, University of Colorado Denver, 1200 Larimer St., Denver, Colorado, 80217 USA*

Abstract

This paper presents a modified current-voltage relationship for the single-diode model. The single-diode model has been derived from the well-known equivalent circuit for a single photovoltaic (PV) cell. A cell is defined as the semiconductor device that converts sunlight into electricity. A PV module refers to a number of cells connected in series and in a PV array, modules are connected in series and in parallel. The modification presented in this paper accounts for both parallel and series connections in an array. Derivation of the modified current-voltage relationships begins with a single solar cell and is expanded to a PV module and finally an array. Development of the modified current-voltage relationship was based on a five-parameter model,

[☆]Corresponding author F. Mancilla–David. Tel. +1–303–556–6674; Fax +1–303–556–2383.

Email addresses: hmtian@szpt.edu.cn (Hongmei Tian), Fernando.Mancilla-David@ucdenver.edu (Fernando Mancilla–David[☆]), kevin.ellis86@gmail.com (Kevin Ellis), eduard.muljadi@nrel.gov (Eduard Muljadi), Peter.Jenkins@ucdenver.edu (Peter Jenkins)

which requires data typically available from the manufacturer. The model accurately predicts voltage-current (V-I) curves, power-voltage (P-V) curves, maximum power point values, short-circuit current and open-circuit voltage across a range of irradiation levels and cell temperatures. The versatility of the model lies in its accurate prediction of the aforementioned criteria for panels of different types, including monocrystalline and polycrystalline silicon. The model is flexible in the sense that it can be applied to PV arrays of any size, as well as in simulation programs such as EMTDC/PSCAD and MatLab/Simulink. The model was used to investigate the effects of shading for different operating conditions to determine the optimal configuration of a PV array. Accuracy of the model was validated through a series of experiments performed outdoors for different configurations of a PV array.

Keywords: Solar Cell, Photovoltaic Module, Photovoltaic Array, PV System Simulation, Mathematical PV Model, Shading Effects

---

Nomenclature

α_T	temperature coefficient of short-circuit current
α'_T	relative temperature coefficient of short-circuit current
β'_T	relative temperature coefficient of open-circuit voltage
β_T	temperature coefficient of open-circuit voltage
γ_C	cell efficiency
$_{ref}$	variable at SRC

E_g bandgap energy, eV

G_T, G solar irradiance/irradiation ($\frac{W}{m^2}$)

I_{dio} current through anti-parallel diode

I_{irr} photocurrent

I_{MP} maximum power point current

I_O diode saturation current

I_p shunt current due to shunt resistor branch

I_{SC} short-circuit current

k Boltzmann's constant ($k = 1.3806503 \times 10^{-23}$ J/K)

n ideality factor

N_C number of cells in series in each module

N_M number of modules in series

N_P number of strings in parallel

N_S number of cells in series

$NOCT$ Nominal Operating Condition ($G_{NOCT} = 800\frac{W}{m^2}, T_{a,NOCT} = 20°C, AM = 1.5$)

q electronic charge ($q = 1.602 \times 10^{-19}$ C)

R_P shunt resistance

R_S series resistance

T cell temperature ($^\circ C$)

$T_{a,NOCT}$ ambient temperature at $NOCT$ conditions ($T_{a,NOCT} = 20^\circ C$)

T_a, T_{amb} ambient temperature ($^\circ C$)

$T_{NOCT}, NOCT$ nominal operating cell temperature ($^\circ C$)

$U_{L,NOCT}$ loss coefficient at $NOCT$ conditions

U_L loss coefficient at operating conditions

V_{MP} maximum power point voltage

V_{OC} open-circuit voltage

$(\tau\alpha)$ absorptance-emittance Product

array any number of modules connected in series and in parallel

cell semiconductor device that converts sunlight into electricity

module any number of solar cells in series

SRC Standard Reference Condition ($G_{ref} = 1000\frac{W}{m^2}, T_{ref} = 25^\circ C$)

1. Introduction

Growing interest in renewable energy resources has caused the photovoltaic (PV) power market to expand rapidly, especially in the area of distributed generation. For this reason, designers need a flexible and reliable

tool to accurately predict the electrical power produced from PV arrays of various sizes. A *cell* is defined as the semiconductor device that converts sunlight into electricity. A *PV module* refers to a number of cells connected in series and in a *PV array*, modules are connected in series and in parallel. Most of the mathematical models developed are based on current-voltage relationships that result from simplifications to the double-diode model proposed by Chan & Phang (1987). The current-voltage relationship for the single-diode model assumes that one lumped diode mechanism is enough to describe the characteristics of the PV cell. This current-voltage relationship is the basis for the mathematical models developed by Desoto et al. (2006) and Jain & Kapoor (2004). Further simplification to the current-voltage relationship is made by assuming the shunt resistance is infinite, thus forming the basis for the four parameter mathematical model. Numerous methods have been developed to solve this particular model. Khezzar et al. (2009) developed three methods for solving the model. Chenni et al. (2007) developed a simplified explicit method by assuming that the photocurrent (I_{irr}) is equal to the short-circuit current (I_{SC}). Zhou et al. (2007) introduced the concept of a Fill Factor (FF) to solve for the maximum power-output (P_{Max}).

Rajapakse & Muthumuni (2009) developed a model based on the current-voltage relationship for the single diode in EMTDC/PSCAD. Campbell (2007) developed a circuit-based, piecewise linear PV device model, which is suitable for use with converters in transient and dynamic electronic simulation software. King (1997) developed a model to reproduce the V-I curve using three important points: short-circuit, open-circuit, and maximum power point conditions on the curve. To improve accuracy, King et al. (2004) expanded the

model to include two additional points along the V-I curve. However, the method requires, in addition to the standard parameters such as the series resistance (R_S) and shunt resistance (R_P), empirically determined coefficients that are provided by the Sandia National Laboratory. The model proposed by King et al. (2004) is ideal for cases where the PV array will be operating at conditions other than the maximum power point.

The U.S. Department of Energy (DOE) supported recent development of the Solar Advisor Model (SAM). SAM provides three options for module performance models: the Sandia Performance Model proposed by King et al. (2004), the five parameter model popularized by Desoto et al. (2006) and a single-point efficiency model. The single-point efficiency model is used for analysis where the parameters required by other models are not available. Cameron et al. (2008) completed a study comparing the three performance models available in SAM with two-other DOE-sponsored models: PVWATTS is a simulation program developed by the National Renewable Energy Laboratory and PVMOD is a simulation program developed by the Sandia National Laboratory. Both programs can be found on the respective laboratory website. The study compared the predicted results with actual measured results from a PV array; all were found to agree with minimal deviation from the measured values. For this study, the modified current-voltage relationship was solved using a method based on the five parameter model since it only requires data provided by the manufacturer and has been shown to agree well with measured results.

In this study, a modified current-voltage relationship for a single solar cell is expanded to a PV module and finally to a PV array. The five parameter

model given by Desoto et al. (2006) uses the current-voltage relationship for a single solar cell and only includes cells or modules in series. This paper presents a modification to this method to account for both series and parallel connections. Detailed current-voltage output functions are developed for a cell, a module and a string of modules connected in series and in parallel. This cell-to-module-to-array model makes the similarities and differences of the equivalent circuits and current-voltage relationships clear.

Manufacturers typically provide the following operational data on PV panels: the open-circuit voltage (V_{OC}); the short-circuit current (I_{SC}); the maximum power point current (I_{MP}) and voltage (V_{MP}); and the temperature coefficients of open-circuit voltage and short-circuit current (β_T and α_T, respectively). This operational data is required to solve the improved five parameter determination method. The model predicted V-I curves, P-V curves, maximum power point, short-circuit current, and open-circuit voltage conditions across a range of irradiation levels and cell temperatures are used for comparison with the experimental data provided by the manufacturer. The proposed model can be applied for PV arrays of any size and is suitable for application in simulation programs such as EMTDC/PSCAD and MatLab/Simulink. A series of experiments were performed outdoors for different configurations of a PV array to validate the accuracy of the model. The experiments revealed consistency between experimental and model predicted results for V-I and P-V curves for each configuration.

Overall, this paper makes the following contributions:

- A current source-based PV array model suitable for computer simulations

- Development of a current-voltage relationship for a PV array
- Development of a datasheet based parameter determination method
- Demonstration of the model and validation through experimental results

2. Development of the Modified Current-Voltage Relationship

Designers need a flexible and reliable tool to accurately predict the electrical power produced from a PV array, whether connected in series or parallel.

2.1. Current-Voltage Relationship for a Single Solar Cell

A solar cell is traditionally represented by an equivalent circuit composed of a current source, an anti-parallel diode, a series resistance and a shunt resistance (Masters (2004)). As shown in Fig. 1, the anti-parallel diode branch is modified to an external control current source which is anti-paralleled with the original current source.

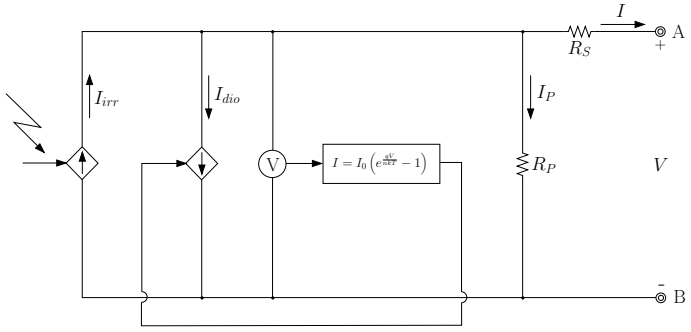

Figure 1: Modified equivalent circuit for a solar cell.

According to Kirchoff's current law,

$$I = I_{irr} - I_{dio} - I_p \tag{1}$$

where I_{irr} is the photo current or irradiance current, which is generated when the cell is exposed to sunlight. I_{irr} varies linearly with solar irradiance for a certain cell temperature. I_{dio} is the current flowing through the anti-parallel diode, which induces the non-linear characteristics of the solar cell. I_p is shunt current due to the shunt resistor R_P branch. Substituting relevant expressions for I_{dio} and I_p, we get

$$I = I_{irr} - I_0 \left[\exp\left(\frac{q\,(V + IR_S)}{nkT} \right) - 1 \right] - \frac{V + IR_S}{R_P} \tag{2}$$

where q is the electronic charge ($q = 1.602 \times 10^{-19}$ C), k is the Boltzmann constant ($k = 1.3806503 \times 10^{-23}$ J/K), n is the ideality factor or the ideal constant of the diode, T is the temperature of the cell, I_0 is the diode saturation current or cell reverse saturation current and R_S and R_P represent the series and shunt resistance, respectively.

2.2. Current-Voltage Relationship for a Photovoltaic Module

A PV module is typically composed of a number of solar cells in series. N_S represents the number of solar cells in series for one module. For example, $N_S = 36$ for BP Solar's BP365 Module, $N_S = 72$ for ET-Solar's ET Black Module ET-M572190BB etc. When N_S solar cells are connected in series to build up a module, the output current I_M and output voltage V_M of the module have the following relationship.

$$I_M = I_{irr} - I_0 \left[\exp\left(\frac{q(V_M + I_M N_S R_S)}{N_S nkT} \right) - 1 \right] - \frac{V_M + I_M N_S R_S}{N_S R_P} \tag{3}$$

This equation can be expanded to any number of cells in series (N_S), and thus is not restricted to one module. If there are N_M modules connected in

series, and there are N_C cells in series in each module, then

$$N_S = N_M \times N_C \tag{4}$$

2.3. Current-Voltage Relationship for a Photovoltaic Array

In an array, PV modules are connected in series and in parallel. It is important to consider the effects of those connections on the performance of the array. We began with the current-voltage relationship for a single solar cell, connected the cells in series to form a string, and now develop the current-voltage relationship for groups of strings connected in parallel (an array). With reference to Fig. 2, the output current I_A and output voltage V_A of a PV array with N_S cells in series and N_P strings in parallel is found from the following equation

$$I_A = N_P I_{irr} - N_P I_0 \left[\exp\left(\frac{q(V_A + I_A \frac{N_S}{N_P} R_S)}{N_S nkT} \right) - 1 \right] - \frac{V_A + I_A \frac{N_S}{N_P} R_S}{\frac{N_S}{N_P} R_P} \tag{5}$$

Comparing (5) with (2), it is clear the equations have similar forms. In electromagnetic transient simulation programs such as EMTDC/PSCAD and MATLAB/SIMULINK, the model of a PV array can be built directly using (5). After adopting the substitutions in Table 1, (5) can be rewritten as

$$I_A = I'_{irr} - I'_0 \left[\exp\left(\frac{q(V_A + I_A R'_S)}{N_S nkT} \right) - 1 \right] - \frac{V_A + I_A R'_S}{R'_P} \tag{6}$$

Following the substitutions outlined in Table 1, the current-voltage relationship given in (6) appears similar to the current-voltage relationship for a single solar cell, and thus the equivalent circuit for the PV array will be similar to the equivalent circuit for a single solar cell (Fig. 1). However,

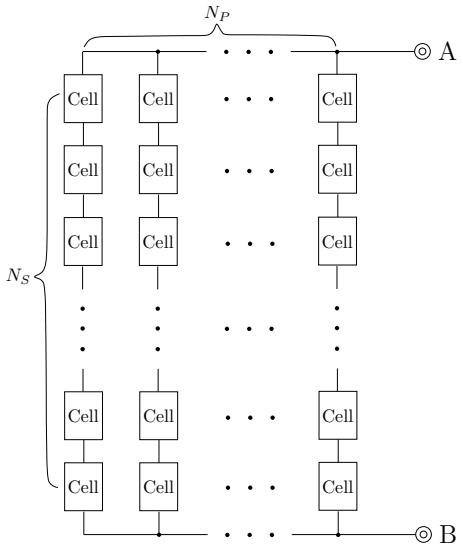

Figure 2: Physical configuration of a PV array

Table 1: Substitutions for the model of a PV array

Original Expression	Substitution
$N_P I_{irr}$	I'_{irr}
$N_P I_0$	I'_0
$\frac{N_S}{N_P} R_S$	R'_S
$\frac{N_S}{N_P} R_P$	R'_P

each variable in the circuit shown in Fig. 1 will now have a different meaning based on the substitutions provided in Table 1 and the second external control current source will have a different control scheme.

3. Important Model Parameters

Prior to derivation of the cell-to-module-to-array model, it is necessary to discuss the important model parameters and how they change with operating conditions.

3.1. Ideality Factor (n)

The ideality factor (n) accounts for the different mechanisms responsible for moving carriers across the junction. The parameter n is 1 if the transport process is purely diffusion and $n \approx 2$ if it is primarily recombination in the depletion region. Some research papers (e.g. Rajapakse & Muthumuni (2009)) suggest an n of 1.3 for silicon. The parameter n represents one of the unknowns of the cell-to-module-to-array model. In our work, n is assumed to be related only to the material of the solar cell and be independent of temperature and solar irradiation.

If values for the photocurrent (I_{irr}), diode saturation current (I_0), series resistance (R_S), and shunt resistance (R_P) are known, along with the operational data provided by the manufacturer (V_{OC}, I_{SC}, I_{MP}, V_{MP}, β_T, α_T), n can be solved for. For example, Jain & Kapoor (2005) used Lambert W-Functions to solve for the ideality factor. Bashahu & Nkundabakura (2007) assessed the accuracy of twenty-two different methods for determining the ideality factor for different current-voltage relationships and described the parameter n as a unitless factor defining the extent to which the solar cell

behaves as an ideal diode. No matter the operating condition, the value of n will not change. The value of n compared to the value of n_{ref} at Standard Reference Conditions (SRC) is given by,

$$n = n_{ref} \tag{7}$$

where the solar irradiation is $G_{ref} = 1000$ W/m^2 and the cell temperature is $T_{ref} = 298$ K or $T_{ref} = 25$°C at SRC.

3.2. Photo Current I_{irr}

The photo current (I_{irr}) depends on the solar irradiance G and cell temperature T and is given by

$$I_{irr} = I_{irr,ref} \left(\frac{G}{G_{ref}} \right) [1 + \alpha'_T (T - T_{ref})] \tag{8}$$

where $I_{irr,ref}$ is the photo current at SRC. α'_T is the relative temperature coefficient of the short-circuit current, which represents the rate of change of the short-circuit current with respect to temperature. Manufacturers occasionally provide the absolute temperature coefficient of the short-circuit current, α_T, for a particular panel. The relationship between α'_T and α_T is

$$\alpha_T = \alpha'_T I_{irr,ref} \tag{9}$$

$I_{irr,ref}$ is the second unknown parameter in the model.

3.3. Diode Saturation Current I_0

I_0 is primarily dependent on the temperature of the cell:

$$I_0 = I_{0,ref} \left[\frac{T}{T_{ref}} \right]^3 \exp \left[\frac{E_{g,ref}}{kT_{ref}} - \frac{E_g}{kT} \right] \tag{10}$$

$I_{0,ref}$, the third unknown parameter in the model, is the diode saturation current for the cell temperature at SRC, T_{ref}. E_g is the bandgap energy [eV]. Kim et al. (2009) defines the value for E_g for silicon to be

$$E_g = 1.16 - 7.02 \times 10^{-4} \left(\frac{T^2}{T - 1108} \right) \tag{11}$$

Fig. 3 shows the relationship between the bandgap energy, E_g, and temperature T.

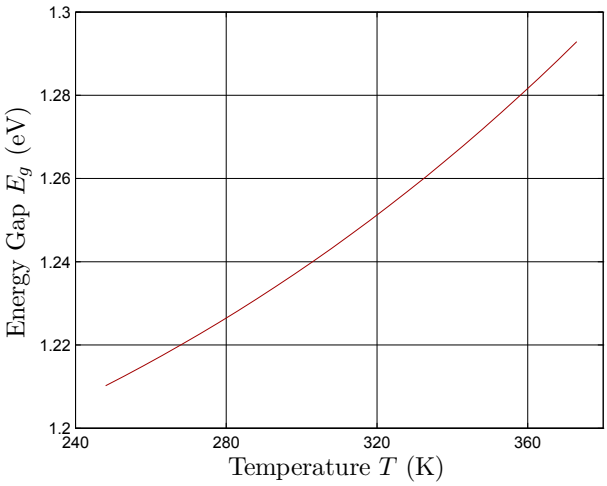

Figure 3: Bandgap energy (E_g) versus temperature

3.4. Temperature of Cell T

Variation in cell temperature occurs due to changes in the ambient temperature as well as changes in the insolation. Masters (2004) defines the cell temperature, T, as:

$$T = T_{amb} + \left(\frac{NOCT - 20°C}{0.8} \right) G \tag{12}$$

where T_{amb} is the ambient temperature and $NOCT$ represents the nominal operating cell temperature provided by the manufacturer. G represents the solar irradiation at the ambient temperature, T_{amb}. Duffie & Beckman (2006) proposed a different formulation for the cell temperature by including heat transfer effects in the form of heat loss coefficients. The cell temperature, T, is given by:

$$\frac{T - T_a}{T_{NOCT} - T_{a,NOCT}} = \frac{G_T}{G_{NOCT}} \frac{U_{L,NOCT}}{U_L} \left[1 - \frac{\eta_c}{(\tau\alpha)}\right] \tag{13}$$

where T_a is the ambient temperature, T_{NOCT} is the nominal operating cell temperature, $T_{a,NOCT} = 20°C$, G_T is the solar irradiation at the ambient temperature, $G_{NOCT} = 800$ W/m^2, $U_{L,NOCT}$ and U_L are the loss coefficients at $NOCT$ and operating temperature conditions respectively, η_c is the efficiency of the cell at the temperature T, and $(\tau\alpha)$ is the absorptance-emittance product. Davis et al. (2001) proposed an equation for the cell temperature T that was derived from an analysis similar to Duffie & Beckman (2006) and is given by

$$T = \frac{G}{G_{NOCT}} (NOCT - T_{ambient,NOCT}) \left(1 - \frac{\eta_c}{\tau\alpha}\right) + T_{ambient} \tag{14}$$

where G is the same as G_T, $NOCT$ is the same as T_{NOCT}, and $T_{ambient,NOCT}$ is the same as $T_{a,NOCT}$. The other variables are identical to those given in (13).

All three equations give similar results for the predicted cell temperature. Calculation of cell temperature using either (13) or (14) is problematic since $(\tau\alpha)$, η_c, $U_{L,NOCT}$ and U_L are rarely known. Thus, for this study (12) will be used.

3.5. Parallel Leakage Resistance R_P and Series Resistance R_S

The parallel leakage resistance or shunt resistance R_P and series resistance R_S are the last two unknown parameters in the cell-to-module-to-array model. As an approximation,

$$R_P > \frac{10V_{OC}}{I_{SC}} \tag{15}$$

where V_{OC} and I_{SC} are open circuit voltage and short circuit current respectively.

Desoto et al. (2006) used the following relationship relating the shunt resistance to irradiation at operating conditions and SRC,

$$\frac{R_P}{R_{P,ref}} = \frac{G}{G_{ref}} \tag{16}$$

Finally,

$$R_S < \frac{0.1V_{OC}}{I_{SC}} \tag{17}$$

In the five parameter method outlined by Desoto et al. (2006), the series resistance is assumed to be independent of temperature and irradiation at both operating conditions and SRC,

$$R_S = R_{S,ref} \tag{18}$$

4. Datasheet Based Parameter Determination Model

In (5), there are five unknown parameters at SRC: $I_{irr,ref}$, $I_{0,ref}$, n_{ref}, $R_{P,ref}$ and $R_{S,ref}$. Solving for these five parameters using the modified current-voltage relationship requires using the mathematical model outlined by Desoto et al. (2006). This model uses data provided by the manufacturer

and as mentioned before agrees well with actual measured results. The data is provided under SRC except for the variable $NOCT$, which is given for nominal operating conditions (800W/m^2 and AM 1.5). Some manufacturers provide data for the panel under nominal operating conditions.

The model is thus a system of five equations with five unknowns. The first equation is derived from open-circuit conditions at SRC where $I_A = 0$ and $V_A = V_{OC,ref}$. Thus (5) becomes

$$0 = N_P I_{irr,ref} - N_P I_{0,ref} \left[\exp\left(\frac{q V_{OC,ref}}{N_S n_{ref} k T_{ref}} \right) - 1 \right] - \frac{V_{OC,ref}}{\frac{N_S}{N_P} R_{P,ref}} \tag{19}$$

The second equation occurs at short-circuit conditions at SRC where $I_A = I_{SC,ref}$, and $V_A = 0$. Thus (5) becomes

$$I_{SC,ref} = N_P I_{irr,ref} - N_P I_{0,ref} \left[\exp\left(\frac{q I_{SC,ref} R_{S,ref}}{N_P n_{ref} k T_{ref}} \right) - 1 \right] - \frac{I_{SC,ref} \frac{N_S}{N_P} R_{S,ref}}{\frac{N_S}{N_P} R_{P,ref}} \tag{20}$$

The measured current-voltage pair at the maximum power point under SRC can be substituted into (5) to obtain the third equation where $I_A = I_{mp,ref}$ and $V_A = V_{mp,ref}$,

$$I_{mp,ref} = N_P I_{irr,ref} - N_P I_{0,ref} \left[\exp\left(\frac{q(V_{mp,ref} + I_{mp,ref} \frac{N_S}{N_P} R_{S,ref})}{N_S n_{ref} k T_{ref}} \right) - 1 \right] - \frac{V_{mp,ref} + I_{mp,ref} \frac{N_S}{N_P} R_{S,ref}}{\frac{N_S}{N_P} R_{P,ref}} \tag{21}$$

At the maximum power point, the derivative of power with respect to voltage is equal to zero. If at SRC, $\frac{\partial P}{\partial v}|_{P=P_{max},SRC} = 0 (P = V_A I_A)$ the fourth equation will be

$$\frac{I_{mp,ref}}{V_{mp,ref}} = \frac{\frac{qN_P I_{0,ref}}{N_S n_{ref} k T_{ref}} \exp\left(\frac{q(V_{mp,ref}+I_{mp,ref}\frac{N_S}{N_P}R_{S,ref})}{N_S n_{ref} k T_{ref}}\right) + \frac{1}{\frac{N_S}{N_P}R_{P,ref}}}{1 + \frac{qI_{0,ref}R_{S,ref}}{n_{ref} k T_{ref}} \exp\left(\frac{q\left(V_{mp,ref}+I_{mp,ref}\frac{N_S}{N_P}R_{S,ref}\right)}{N_S n_{ref} k T_{ref}}\right) + \frac{R_{S,ref}}{R_{P,ref}}} \tag{22}$$

The fifth and final equation ensures that the temperature coefficient of open-circuit voltage (β_T) is correctly predicted by the model,

$$\beta_T = \frac{\partial V_{OC}}{\partial T} \qquad \frac{V_{OC} - V_{OC,ref}}{T - T_{ref}} \tag{23}$$

$$V_{OC} = V_{OC,ref} + \beta_T (T - T_{ref}) \tag{24}$$

β_T is the absolute temperature coefficient of the open-circuit voltage. Some manufacturers only provide the relative temperature coefficient of the open-circuit voltage, β'_T. The relationship between them is given by

$$\beta_T = \beta'_T V_{OC,ref} \tag{25}$$

In equation (24), the variable V_{OC} represents the open-circuit condition at the cell temperature T. A cell temperature of $T = T_{ref} \pm 10$ K should be used, since choosing 1 to 10K above or below T_{ref} results in the same answer. Now, V_{OC} at some cell temperature T can be obtained from (5) using the same method in deriving (19). Thus,

$$0 = N_P I_{irr} - N_P I_0 \left[\exp(\frac{qV_{OC}(T)}{N_S n k T}) - 1\right] - \frac{V_{OC}(T)}{\frac{N_S}{N_P}R_P} \tag{26}$$

The variables I_{irr}, I_0, R_P, n are the photocurrent, diode saturation current, and shunt resistance at the cell temperature T, respectively. When

solving for the reference parameters ($I_{irr,ref}$, $I_{0,ref}$, n_{ref}, $R_{P,ref}$, $R_{S,ref}$) the solar irradiation is assumed equal ($G = G_{ref}$). We make the following substitutions in (26): (8) for I_{irr}, (10) and (11) for I_0, (16) for R_P, (7) for n, and the term $V_{OC}(T)$ from (24). After the necessary substitutions, the fifth and final condition can be written in terms of the reference parameters only.

The five equations (19), (20), (21), (22), and (26) can now be solved simultaneously for the five parameters at reference conditions. These equations were solved using the nonlinear equation solver fsolve in MatLab. Once all of the parameters at reference conditions are obtained, the cell-to-module-to-array model can predict the performance of an array of any size under different operating conditions.

Sometimes it is desirable to find the short-circuit current, and the voltage and current at the maximum power point, under cell temperature and irradiation values different from reference conditions. The short-circuit current at any operating condition is given by,

$$I_{SC} = N_P I_{irr} - N_P I_0 \left[\exp\left(\frac{qI_{SC}R_S}{N_P nkT}\right) - 1\right] - \frac{I_{SC}R_S}{R_P} \tag{27}$$

Maximum power point current and voltage at any operating condition can be obtained by simultaneously solving the following two equations using fsolve in MatLab/Simulink,

$$I_{mp} = N_P I_{irr} - N_P I_0 \left[\exp\left(\frac{q(V_{mp} + I_{mp}\frac{N_S}{N_P}R_S)}{N_S nkT}\right) - 1\right] - \frac{V_{mp} + I_{mp}\frac{N_S}{N_P}R_S}{\frac{N_S}{N_P}R_P} \tag{28}$$

$$\frac{I_{mp}}{V_{mp}} = \frac{\frac{qN_P I_0}{N_S nkT} \exp\left(\frac{q(V_{mp}+I_{mp}\frac{N_S}{N_P}R_S)}{N_S nkT}\right) + \frac{1}{\frac{N_S}{N_P}R_P}}{1 + \frac{qI_0 R_S}{nkT} \exp\left(\frac{q\left(V_{mp}+I_{mp}\frac{N_S}{N_P}R_S\right)}{N_S nkT}\right) + \frac{R_S}{R_P}} \tag{29}$$

5. Results

The cell-to-module-to-array model was tested for twenty panels, and yielded results consistent with experimental data provided by manufacturers under a wide range of cell temperatures and irradiation values. For brevity, the results for three PV modules are provided here. The modules include BP Solar's BP 3 Series 235W PV module, ET Solar's ET Black Module ET-M572190BB, and Kyocera's KD210GX-LP high efficiency multicrystal PV module.

Table 2 presents the calculated reference parameters for the BP 3 Series 235W, ET-M572190BB and KD210GX-LP modules. Due to the nonlinear nature of the equations, the simulation results for a PV array are particularly sensitive to the values of the parameters at reference conditions. Without accurate reference parameters, it is impossible to define the characteristics of the V-I curve for operating conditions. The parameters in Table 2 have an explicit physical meaning intrinsic to a specific PV panel.

Figure 4 presents the model V-I curves for BP Solar's BP 3 Series 235 W panel at a cell temperature of 25°C and solar irradiation at five levels: 1000 W/m^2; 800 W/m^2; 600 W/m^2; 400 W/m^2; and 200 W/m^2. The V-I curves and values for the short-circuit current and open-circuit voltage compare favorably with published values.

Figure 6 presents the V-I curves produced from the model for BP Solar's

Table 2: This table was merged and is now part of Table 2

Reference	BP 3 Series		
Parameters	215 W	225 W	235 W
$I_{irr,ref}$	8.122	8.310	8.487
$I_{0,ref}$	6.012×10^{-9}	6.192×10^{-9}	6.330×10^{-9}
$R_{S,ref}$	0.005649	0.005697	0.005125
$R_{P,ref}$	2.093	4.865	5.837
n_{ref}	1.128	1.130	1.149

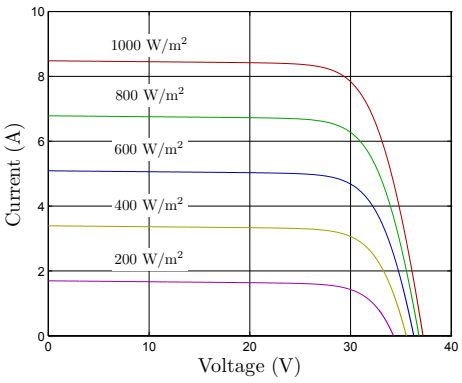

Figure 4: Current vs. Voltage curves for BP Solar's BP 3 Series 235 W PV module at a cell temperature of 25°C and solar irradiation at five levels: 1000 W/m^2; 800 W/m^2; 600 W/m^2; 400 W/m^2; and 200 W/m^2

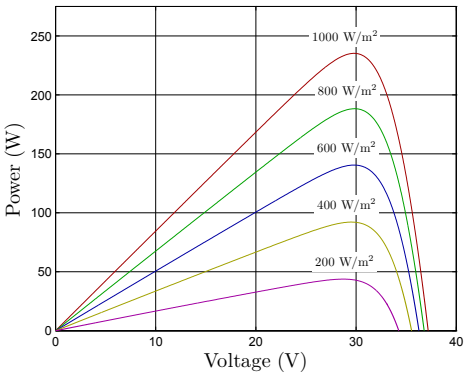

Figure 5: This figure was deleted

BP 3 Series 235 W panel at the same irradiation level of 1000 W/m^2, but with varying cell temperatures: 0°C; 25°C; 50°C; and 75°C. The model results are again consistent with published values.

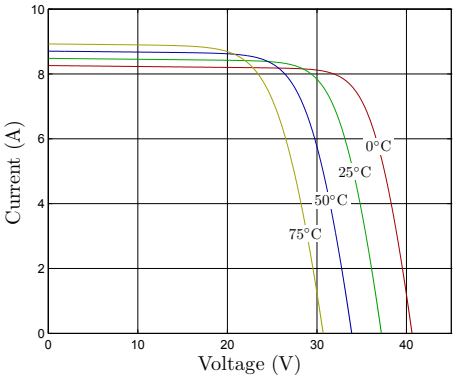

Figure 6: Current vs. Voltage curves for BP Solar's BP 3 Series 235 W PV panel at an irradiation level of 1000 W/m^2 and cell temperatures: 0°C; 25°C; 50°C; and 75°C

To check the model's ability to predict the output power and values for V_{OC} and I_{SC}, further calculations were made under both reference conditions (SRC) and nominal operating conditions (NOCT). Table 3 compares the

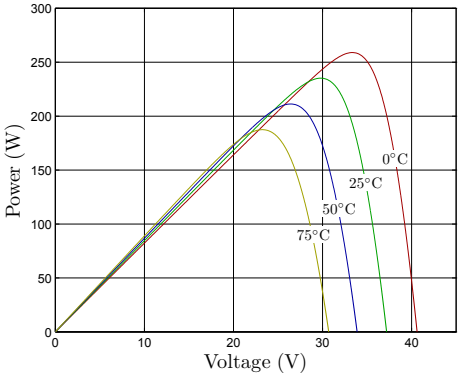

Figure 7: This figure was deleted

model values for P_{max}, I_{mp}, V_{mp}, V_{OC} and I_{SC} with values published by the manufacturers.

For ET Solar's ET-M572190BB PV module, Figure 6 presents V-I and P-V curves at a fixed cell temperature of 25°C and different irradiation levels. The maximum power point for each condition is given on each curve and the numerical results are published in Table 4. Comparison between these calculated maximum power point values and those published by the manufacturer reveals that they are in good agreement.

The cell-to-module-to-array model provides designers with a reliable and accurate method for predicting the performance of PV arrays of any size and under different operating conditions. Energy production, efficiency, maximum power, maximum power point voltage and current, short-circuit current, and open-circuit voltage are all predicted accurately for differing irradiation levels and cell temperatures. Our results reveal that through accurate calculation of reference parameters, the model can predict the V-I and P-V curves for any size array.

Table 3: This table was deleted

Operating Conditions	Parameter	BP 3 Series 215 W		220 W	
		Datasheet	Model	Datasheet	Model
	P_{max} (W)	215	215.34	220	219.64
SRC	V_{mp} (V)	29.1	29.10	28.9	28.90
1000 W/m^2	I_{mp}(A)	7.4	7.40	7.6	7.60
25°C	V_{CO} (V)	36.5	36.50	36.6	36.60
	I_{SC} (A)	8.10	8.10	8.20	8.20
	P_{max} (W)	154.8	156.62	158	160.25
NOCT	V_{mp} (V)	25.9	26.21	25.7	26.07
800 W/m^2	I_{mp} (A)	5.92	5.976	6.08	6.15
47°C	V_{CO} (V)	33.2	33.20	33.3	33.30
	I_{SC} (A)	6.56	6.63	6.64	6.71

Table 4: This table was merged and is now part of Table 3

Operating Conditions	Parameter	BP 3 Series 225 W Datasheet	225 W Model	235 W Datasheet	235 W Model
	P_{max} (W)	225	224.07	235.12	235.12
SRC	V_{mp} (V)	29.1	29.10	29.8	29.8
1000 W/m^2	I_{mp}(A)	7.70	7.70	7.89	7.89
25°C	V_{CO} (V)	36.6	36.60	37.2	37.2
	I_{SC} (A)	8.30	8.30	8.48	8.48
	P_{max} (W)	162	163.34	169.2	171.3
NOCT	V_{mp} (V)	25.9	26.23	26.5	26.84
800 W/m^2	I_{mp} (A)	6.16	6.23	6.31	6.38
47°C	V_{CO} (V)	33.3	33.30	33.8	33.85
	I_{SC} (A)	6.72	6.79	6.87	6.94

Table 5: This table was merged and is now part of Table 2

Reference Parameters	ET-M572190BB
$I_{irr,ref}$	5.565
$I_{0,ref}$	1.774×10^{-9}
$R_{S,ref}$	0.006946
$R_{P,ref}$	7.287
n_{ref}	1.118

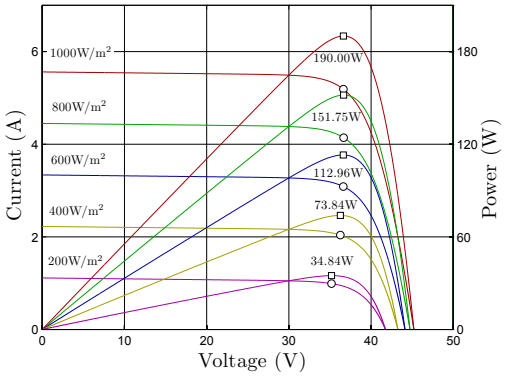

Figure 8: Current vs. Voltage and Power vs. Voltage curves for the ET-M572190BB PV module at a cell temperature of 25°C and solar irradiation at five levels: 1000 W/m^2; 800 W/m^2; 600 W/m^2; 400 W/m^2; and 200 W/m^2

Table 6: Predicted maximum power point values and published results for ET-M572190BB PV panel at a cell temperature of 25°C and solar irradiation at five levels: 1000 W/m^2; 800 W/m^2; 600 W/m^2; 400 W/m^2; and 200 W/m^2

Irradiation (G) (W/m^2)	ET-M572190BB Datasheet	Maximum Power (W) Model
1000	190.2	190.00
800	150.8	151.75
600	111.4	112.96
400	72.2	73.84
200	33.6	34.84

Table 7: This table was deleted

Reference Parameters	Sunpower 215
$I_{irr,ref}$	5.807
$I_{0,ref}$	2.946×10^{-10}
$R_{S,ref}$	0.00625
$R_{P,ref}$	4.957
n_{ref}	1.102

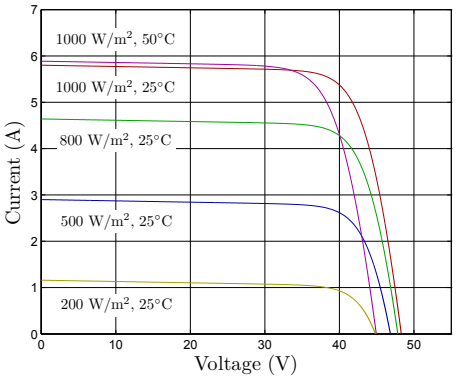

Figure 9: This figure was deleted

Table 8: This table was merged and is now part of Table 2

Reference Parameters	KD210GX-LP
$I_{irr,ref}$	8.596
$I_{0,ref}$	6.230×10^{-9}
$R_{S,ref}$	0.00503
$R_{P,ref}$	2.7106
n_{ref}	1.138

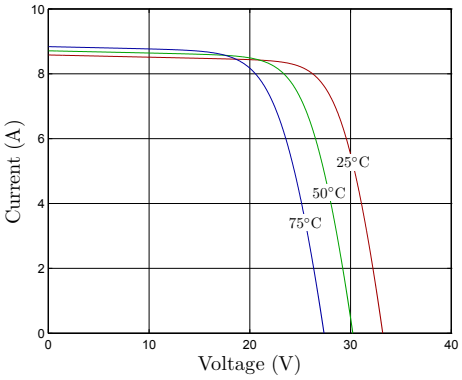

Figure 10: This figure was deleted

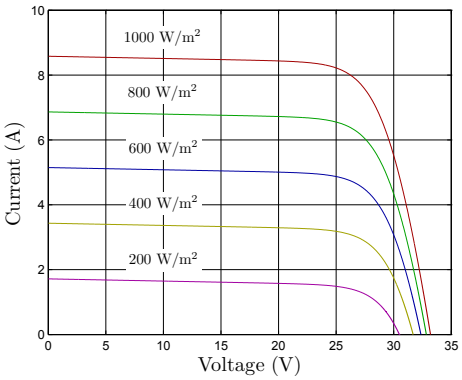

Figure 11: This figure was deleted

Table 9: This table was merged and is now part of Table 3

Operating Condition	Parameter	Kyocera Datasheet	KD210GX-LP Model
	P_{max} (W)	210	210.14
SRC	V_{mp} (V)	26.6	26.60
1000 W/m^2	I_{mp}(A)	7.90	7.90
25°C	V_{CO} (V)	33.2	33.20
	I_{SC} (A)	8.58	8.58
	P_{max} (W)	148	149.96
NOCT	V_{mp} (V)	23.5	23.72
800 W/m^2	I_{mp} (A)	6.32	6.32
49°C	V_{CO} (V)	29.9	29.96
	I_{SC} (A)	6.98	6.96

The modified equivalent circuit and current-voltage relationship can be easily transferred into simulation programs such as EMTDC/PSCAD and MatLab/Simulink. In EMTDC/PSCAD, the PV array model was created through a user-defined module using standard software library components. The process is straightforward and further connection with other ancillary power components that comprise the entire system is easily accomplished.

6. Shading Effects

The model can also be used to investigate the effects of shading of a PV array and determine the optimal configuration depending on the number of bypass diodes of the PV module composing the array. (Aside: bypass diodes are solid state devices made of P-type and N-type silicon.) In a PV module, all the cells are connected in series, thus the same current must flow through each cell. The shaded cells operate at a current higher than their short-circuit current which occurs at negative voltage, thus yielding negative power. The shaded cells will dissipate power as heat and cause "hot spots." Bypass diodes allow current to pass around shaded cells thereby reducing the voltage losses of the system.

To illustrate the role of the bypass diode, consider the performance of the BP 3 Series 235 W PV module under the following three conditions: 1 the entire module is unshaded; 2 one cell in the module is completely shaded with and without a bypass diode; 3 two cells in the module are completely shaded with and without a bypass diode. Figure 12 and Figure 13 show the current-voltage and power-voltage curves for these conditions. Simply shading one cell of the module causes performance to decrease; shading two is even worse.

Clearly, the bypass diode mitigates the effects of shading. In either case of having one or two cells shaded, when those cells are connected in parallel with a bypass diode the current-voltage and power-voltage curves resemble the curves of the unshaded condition, thus the bypass diode has been shown to improve the power produced and prevent the "hot spots" problem.

A PV module will operate most efficiently if a bypass diode is connected in parallel with every cell. However, this is impractical from a design perspective and manufacturers typically provide three bypass diodes for the PV module, such as for the Kyocera KC85TS PV module, where one bypass diode must be connected in parallel to a group of cells. At least one bypass diode is added to protect the module and preserve the integrity of the array.

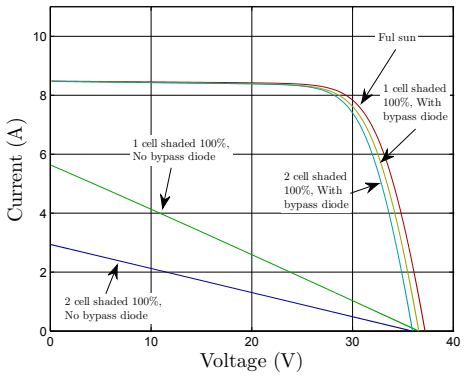

Figure 12: V-I curves for the BP 3 Series 235 W PV module under five conditions: unshaded (G = 1000 W/m^2); one cell shaded with and without a bypass diode; two cells shaded with and without a bypass diode. The cell temperature is 25°C

In a large PV array, modules often operate under different conditions; some modules may experience different irradiation levels or cell temperatures due to changes in ambient temperatures across the array. The EMTDC/PSCAD

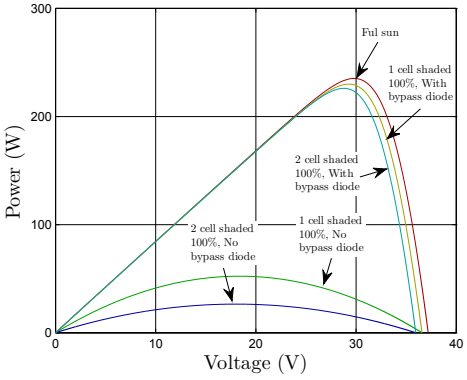

Figure 13: Power-voltage curves for the BP 3 Series 235 W PV module under five conditions: unshaded ($G = 1000$ W/m^2); one cell shaded with and without a bypass diode; two cells shaded with and without a bypass diode. The cell temperature is 25°C

model provides a convenient way to investigate such effects and determine an optimal configuration (in terms of series and parallel connections to maximize power production). If the model could be used in conjunction with a controllable switching matrix, a PV array could continuously maintain that optimal configuration. Velasco-Quesada et al. (2009) reconfigured a grid-connected PV system to improve energy production by using a controllable switching matrix to maintain the system at the optimal configuration. Consider a simple PV array composed of four BP 3 Series 235 W PV modules. An array of this size can have five different configurations, as shown in Figure 14.

Configurations I and II describe arrays where all the modules are connected in either series or parallel, respectively. Configuration III describes an array where there are two strings, modules 1 and 2 connected in series and modules 3 and 4 connected in series, connected in parallel. Configurations IV and V are similar however the strings have different modules connected

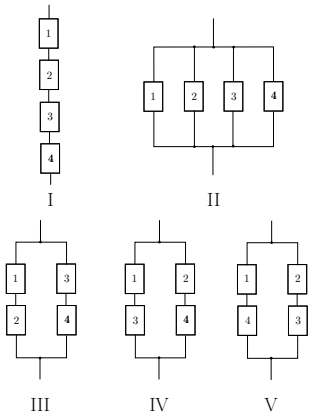

Figure 14: Possible configurations of a PV array composed of four PV modules

in series. To investigate the shading effects, different cases are considered where each module of the various configurations shown in Figure 14 operates at a different value of irradiation or cell temperature. In each case the effect of the bypass diode is investigated as well by considering the condition where each module has either no bypass diode or one bypass diode.

Three different cases are considered: 1 each module operates at the same cell temperature, but at a different irradiation level (Table 10); 2 each module operates at the same irradiation, but at different cell temperatures (Table 12); 3 each modules operates at a different irradiation and cell temperature (Table 14). Each of the possible configurations will result in a different maximum power point assuming the array operates at the maximum power point.

6.1. Case 1

For the first case, four PV modules experience irradiation levels of 400 W/m^2, 600 W/m^2, 800 W/m^2 and 1000 W/m^2 respectively (module number corresponds to the module shown in Figure 14), with a cell temperature of

25°C. The voltage of each module will remain the same (function of cell temperature), however the current will be different (function of irradiation).

Table 10: Case 1

Module	G (W/m^2)	T (°C)
1	400	25
2	600	25
3	800	25
4	1000	25

Figure 15 and Figure 16 give the current-voltage and power-voltage curves for the five configurations without the bypass diode. Configuration II (all modules connected in parallel) produces the most power and Configuration I (all modules connected in series) produces the least. For this case, since the current is a function of irradiation, the optimal configuration is connecting the modules in parallel.

Manufacturers always include at least one bypass diode to protect the module. Suppose that each BP 3 Series 235 W PV module has one bypass diode. Figure 17 and Figure 18 show the current-voltage and power-voltage curves for the five configurations with each module having one bypass diode. Comparing Figure 15 with Figure 17 and Figure 16 with Figure 18, both the current-voltage and power-voltage curves shift upward relative to the case without a diode. The maximum power of Configuration I increases from 415.06 W in Figure 16 to 459.92 W in Figure 18. The values for the current and power increase for the other configurations as well. Recall that since the

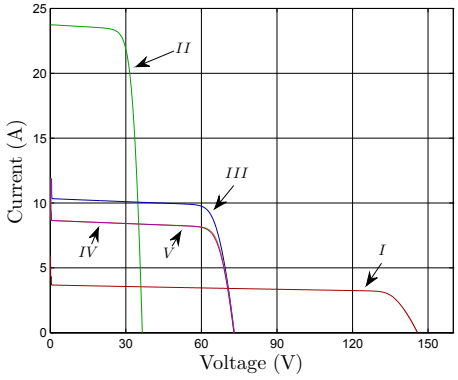

Figure 15: Case 1: V-I curves for the five configurations without a bypass diode for each module

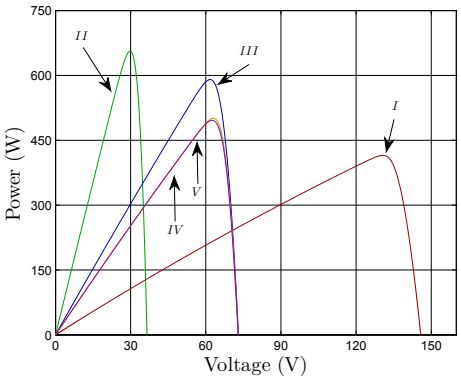

Figure 16: Case 1: Power-voltage curves for the five configurations without a bypass diode for each module

ideal situation is to have each solar cell connected in parallel with a bypass diode, the power and current can only increase by increasing the number of bypass diodes.

Table 11 gives the power produced for each configuration where each module has one bypass diode. Depending on the configuration the power produced will change. In this case, the optimal configuration is Configuration

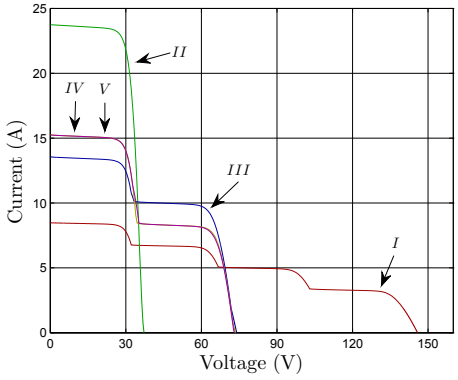

Figure 17: Case 1: V-I curves for the five configurations with a bypass diode for each module

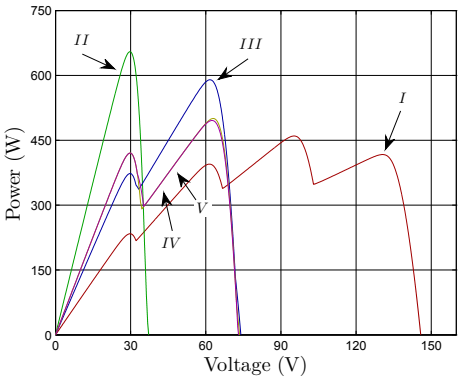

Figure 18: Case 1: Power-voltage curves for the five configurations with a bypass diode for each module

II.

6.2. Case 2

For the second case, four PV modules experience cell temperatures of -5°C, 0°C, 5°C and 80°C with an irradiation level of 1000 W/m^2. As mentioned previously, the voltage of each module will vary as a function of cell

Table 11: Case 1: Maximum power produced for each configuration

Configuration	P_{max} (W)
I	459.92
II	654.78
III	589.91
IV	500.33
V	495.82

temperature, but the current will remain the same.

Table 12: Case 2

Module	G (W/m^2)	T (°C)
1	1000	-5
2	1000	0
3	1000	5
4	1000	80

Figure 19 and Figure 20 give the current-voltage and power-voltage curves for each configuration where each module has one bypass diode. Configuration I produces the most power and Configuration II the least. Configurations III, IV, and V produce nearly the same power. For this case, since the voltage is a function of cell temperature, the optimal configuration is connecting the modules in series.

Table 13 gives the power produced for each configuration. In this case,

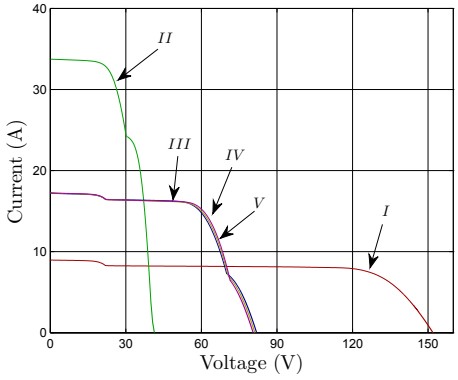

Figure 19: Case 2: V-I curves for the five configurations with a bypass diode for each module

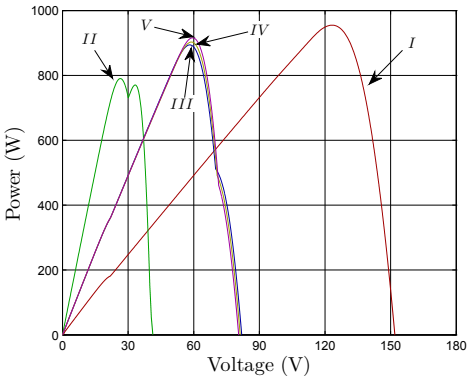

Figure 20: Case 2: Power-voltage curves for the five configurations with a bypass diode for each module

the optimal configuration is Configuration I and Configurations III, IV, and V produce nearly the same power.

6.3. Case 3

The third case considers each module operating under a different cell temperature and irradiation level (Table 14).

Table 13: Case 2: Maximum power produced for each configuration

Configuration	P_{max} (W)
I	954.88
II	790.27
III	894.01
IV	902.90
V	915.89

Table 14: Case 3

Module	G (W/m^2)	T (°C)
1	750	-1
2	1050	57
3	860	77
4	1160	33

Figure 21 and 22 give the current-voltage and power-voltage curves for each configuration where each module has one bypass diode. The optimal configuration for this case is Configuration IV and Configuration V will produce the least power.

Table 15 gives the power produced for each configuration where each module has one bypass diode. For this case, the optimal configuration is Configuration IV.

It is interesting to note that by including a bypass diode for each module,

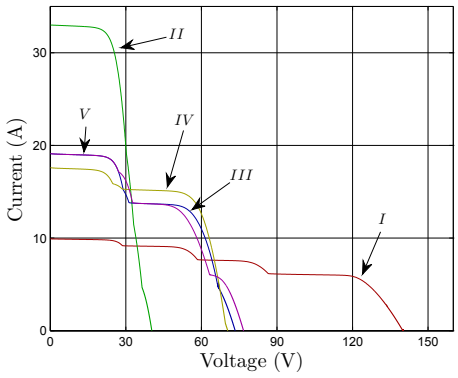

Figure 21: Case 3: V-I curves for the five configurations with a bypass diode for each module

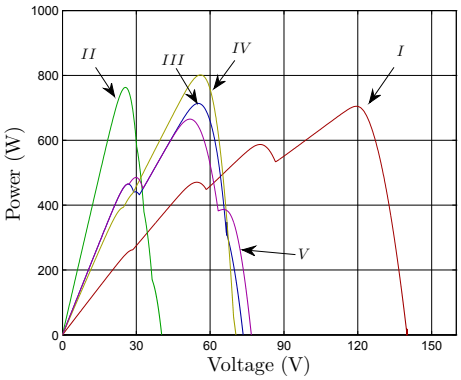

Figure 22: Case 3: Power-voltage curves for the five configurations with a bypass diode for each module

the V-I curve exhibits step behavior and the power-voltage curve has multiple extrema (Figures 15-22). With additional bypass diodes, both curves will become more smooth and the maximum power of the array will increase.

The model presents a convenient method for investigating the effects of shading on the performance of a PV array. Depending on the scale of the PV array, the overall array can be divided into multiple sub-arrays that

Table 15: Case 3: Maximum power produced for each configuration

Configuration	P_{max} (W)
I	704.86
II	762.98
III	713.67
IV	801.57
V	665.24

operate under similar conditions. The extent of shading on a sub-array, which directly affects the irradiation and cell temperature, can be adjusted easily in EMTDC/PSCAD and the optimal configuration then deduced from the model.

7. Experiment

Experiments were performed outdoors using four Kyocera's KC85TS PV modules installed on the roof of the North Classroom building at the University of Colorado Denver campus. A photo of the experimental setup is presented in Figure 23. The objective was to confirm that the cell-to-module-to-array model could accurately replicate outdoor conditions for different configurations of a PV array. Solar irradiation levels were measured using the LI-COR model 200SA pyranometer and cell temperature was measured by a thermocouple attached to the rear surface of the PV module. A simple thermometer monitored the ambient temperature. Data was collected every second and averaged for the minute using a CR-10X datalogger. For

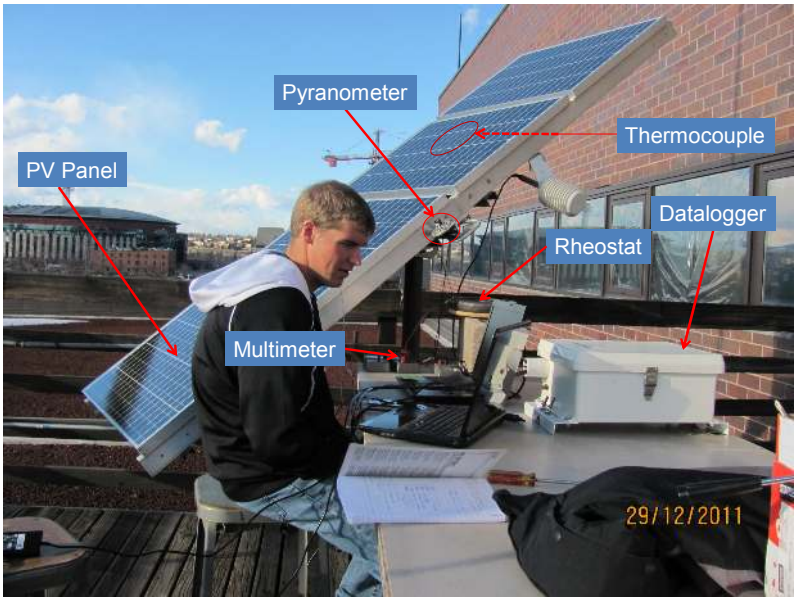

Figure 23: Experimental device and circuit of outdoor measurement.

the experiment, measurement of the V-I curve for different configurations of the four panel array was achieved through a variable resistor method. An Ohmite 45 Ohm 1000 W rheostat was used to replicate the load of the array. Through variation of the resistance of the rheostat, different points on the V-I curve were captured using multimeters to measure the current and voltage at each point.

The experiment revealed that the specifications (P_{max}, V_{mp}, I_{mp}, I_{SC}, V_{OC}, α_T) provided by the manufacturer could not be used in the cell-to-module-to-array model to accurately replicate outdoor conditions. Possible reasons could be the method of manufacture or the age of the module. Instead, the specifications for one module of the system were calculated under an outdoor reference condition (different from SRC) and used as input for

the model. Figure 24 represents the V-I curve for one module under the outdoor reference condition of $G = 967.71$ W/m^2, $T = 308.82$ K.

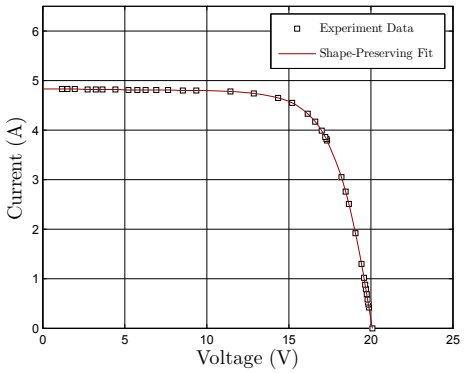

Figure 24: V-I curve for one Kyocera KC85TS module under the outdoor reference condition of $G = 967.71$ W/m^2, $T = 308.82$ K

Based on this curve, the necessary specifications were calculated (Table 16) and assumed to be representative of each of the four modules in the system.

In order to estimate the temperature coefficient of I_{SC} (α_T), the short-circuit current was measured on a clear day (Jan 5, 2012) from 9:35 AM to 12:32 PM. Figure 25 reveals the tendency of the relative short-circuit current to change due to changes in solar irradiation.

The results reveal a linear relationship between short-circuit current and solar irradiation. Rearrangement of (8) led to the relationship between $\frac{I_{SC}}{I_{SC,ref}} \times \frac{G_{ref}}{G}$ and $T - T_{ref}$ as shown in Figure 26. In this case, "ref" refers to the outdoor reference condition.

The slope of the line represents the relative temperature coefficient α'_T. From Figure 26, it is reasonable to consider α'_T as zero and thus α_T as zero.

Table 16: Calculated specifications for one Kyocera KC85TS module under the outdoor reference condition of $G = 967.71$ W/m^2, $T = 35.62$°C (308.82 K) and ambient temperature $T_a = 14.69$°C (287.89 K).

Specification	Calculated Value
Maximum Power, P_{max} (W)	69.99
Voltage at Maximum Power, V_{mp} (V)	15.96
Current at Maximum Power, I_{mp} (A)	4.382
Short-Circuit Current, I_{SC} (A)	4.83
Open-Circuit Voltage, V_{OC} (V)	20.09
Temperature Coefficient of I_{SC}, α_T (A/°C)	0
Temperature Coefficient of V_{OC}, β_T (V/°C)	-0.0821
Number of Solar cells in Series, N_S	36
Number of Solar cells in Parallel, N_P	2

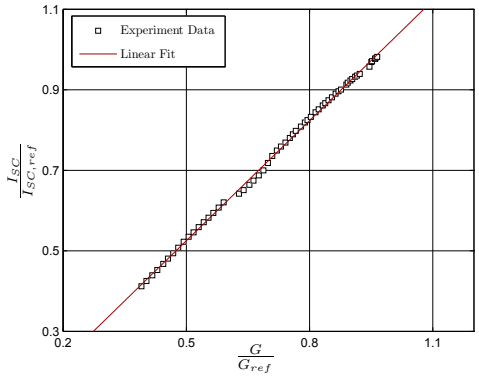

Figure 25: Relative short-circuit current versus relative solar irradiation under outdoor condition.

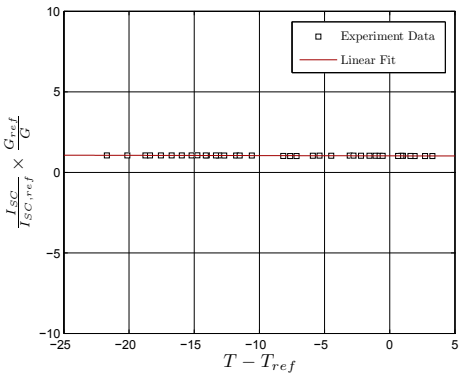

Figure 26: Relationship between $\frac{I_{SC}}{I_{SC,ref}} \times \frac{G_{ref}}{G}$ and $T - T_{ref}$ where the slope is α'_T under the outdoor condition

The temperature coefficient of V_{OC} (β_T) represents the value provided by the manufacturer.

Based on the specifications given in Table 16, the reference parameters shown in Table 17 were calculated using the cell-to-module-to-array model.

Table 17: Reference parameters for the Kyocera KC85TS module where "ref" refers to the outdoor reference condition

Reference Parameter	Calculated Value
$I_{irr,ref}$	2.4207
$I_{0,ref}$	1.996×10^{-8}
$R_{S,ref}$	0.01526
$R_{P,ref}$	6.4616
n_{ref}	1.1287

After obtaining the reference parameters, comparisons between results

of the outdoor experiments and the cell-to-module-to-array model were performed for three different cases: 1) PV modules wired only in parallel, including 2 modules in parallel, 3 in parallel, and 4 in parallel; 2) PV modules wired only in series, including 2 modules in series, 3 in series, and 4 in series; 3) PV modules wired in both series and parallel (2 strings of 2 modules in series in parallel).

For the first case, Figure 27 and Figure 28 reveal the V-I and P-V curves respectively for each instance of parallel configuration as well as the respective curves for one module.

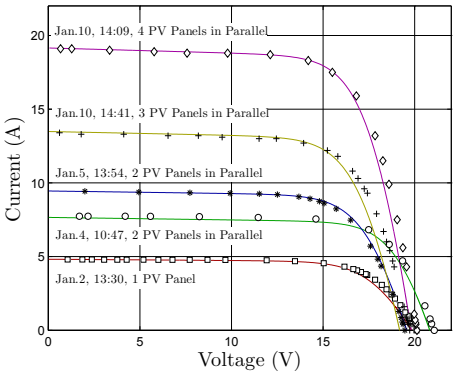

Figure 27: Case 1: V-I curve comparison between experimental results (scattered points) and model results (solid line)

Figure 27 and Figure 28 reveal consistency between experimental results (scattered points) and model results (solid line). The corresponding solar irradiation and cell temperature for each experiment are shown in Table 18 as well as the time and date of each experiment.

For the second case, Figure 29 and Figure 30 show the V-I and P-V curves respectively for each instance of series configuration as well as two instances

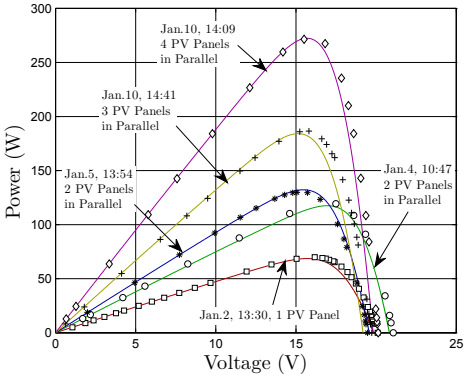

Figure 28: Case 1: P-V curve comparison between experimental results (scattered points) and model results (solid line)

Table 18: Case 1: Date, time, solar irradiation and cell temperature for each experiment

Date	Time	Configuration	G (W/m^2)	T (K)
Jan 2, 2012	1:30 PM	1 Module	965.68	311.84
Jan 4, 2012	10:47 AM	2 Modules in Parallel	767.15	296.93
Jan 5, 2012	1:54 PM	2 Modules in Parallel	946.68	314.84
Jan 10, 2012	2:41 PM	3 Modules in Parallel	900.59	318.84
Jan 10, 2012	2:09 PM	4 Modules in Parallel	959.21	312.07

for one module.

Figure 29 and Figure 30 reveal consistency between experimental results (scattered points) and model results (solid line). The difference around the open-circuit voltage point in either case is due to the uncertainty of the temperature coefficient of V_{OC} (β_T). Recall that the value provided by the manufacturer was adopted for the model, which introduces some discrepancy

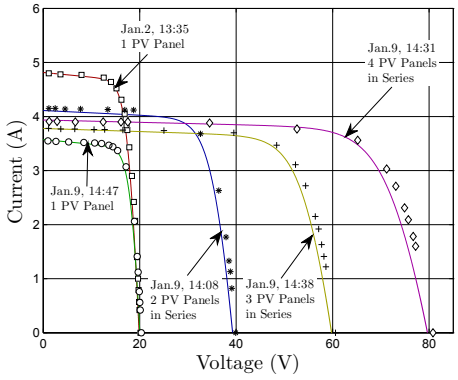

Figure 29: Case 2: V-I curve comparison between experimental results (scattered points) and model results (solid line)

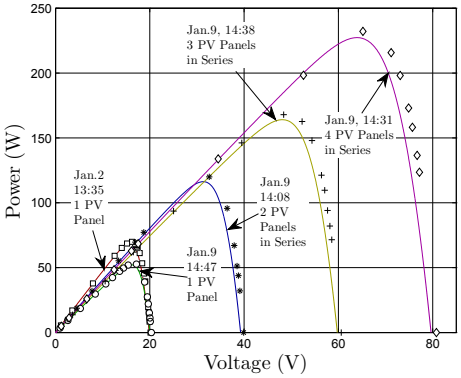

Figure 30: Case 2: P-V curve comparison between experimental results (scattered points) and model results (solid line)

since a "used" PV module is (to some extent) different from a "new" one. The accuracy of predicted results could be improved with a temperature coefficient of V_{OC} characteristic of the PV module. The corresponding solar irradiation and cell temperature, along with the time and date, are shown for each experiment in Table 19.

Table 19: Case 2: Date, time, solar irradiation and cell temperature for each experiment

Date	Time	Configuration	G (W/m^2)	T (K)
Jan 2, 2012	1:35 PM	1 Module	964.58	311.45
Jan 9, 2012	2:47 PM	1 Module	716.05	305.52
Jan 9, 2012	2:08 PM	2 Modules in Series	823.67	312.19
Jan 9, 2012	2:38 PM	3 Modules in Series	757.12	307.49
Jan 9, 2012	2:30 PM	4 Modules in Series	788.49	308.17

For the third case, Figure 31 and Figure 32 show the V-I and P-V curves respectively for PV modules wired in both series and parallel (2 strings of 2 modules in series in parallel). Once again, consistency between experimental results (scattered points) and model results (solid line) is shown.

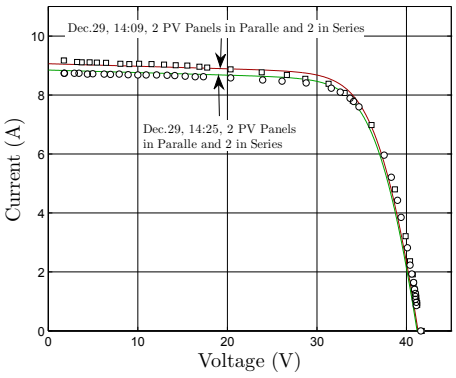

Figure 31: Case 3: V-I curve comparison between experimental results (scattered points) and model results (solid line)

Table 20 shows the corresponding information for each experiment.

It is clear that the model accurately predicts the V-I and P-V curves for

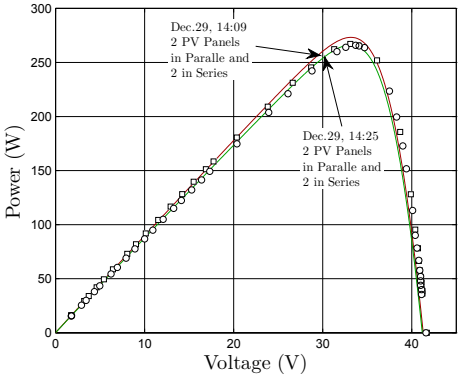

Figure 32: Case 3: P-V curve comparison between experimental results (scattered points) and model results (solid line)

Table 20: Case 3: Date, time, solar irradiation and cell temperature for each experiment

Date	Time	Configuration	G (W/m^2)	T (K)
Dec 29, 2011	2:09 PM	2 in Series 2 in parallel	907.72	301.30
Dec 29, 2011	2:25 PM	2 in Series 2 in parallel	886.22	301.58

different configurations, and thus is able to address the variation in outdoor conditions imparted by shading effects. For example, it can be beneficial to connect PV modules in parallel depending on shading effects. When the solar irradiation level is not uniform throughout the array, the contributions to the current from each PV module will be different; if connected in parallel, the different currents will not offset each other, thereby increasing overall power. In EMTDC/PSCAD a module can be defined to represent a PV array, thus adding to the convenience of simulating any sized PV array. The agreement between experimental results and model predicted results reveals

the reliability and accuracy of the model.

8. Conclusion

A modified equivalent circuit and current-voltage relationship to include the effects of parallel and series connections in a PV array was derived using the single diode model for a single solar cell. This was expanded to a string of any number of cells in series and finally to an array. Modification to the five parameter model was made because of the current-voltage relationship derived for an array, and this resulted in development of a cell-to-module-to-array model. The flexibility of this model derives from its ability to produce all important parameters and V-I and P-V for arrays of any size. The accuracy of the model was demonstrated by a systematic comparison of model results and published data provided by panel manufacturers. The model requires information that is typically available to the designer. Model flexibility, accuracy and ease of use thus combine to give the designer a reliable prediction tool under a wide range of conditions. The modified equivalent circuit is easily used in simulation programs such as EMTDC/PSCAD and MatLab/Simulink. Validation of the accuracy of the model was shown through a series of experiments performed outdoors for different configurations of a PV array. The consistency between V-I and P-V curves for experimental and model predicted results for each configuration revealed the reliability and accuracy of the model.

9. Acknowledgment

We would like to thank Thomas Stoffel and Afshin Andreas at the Solar Radiation Research Laboratory from the National Renewable Energy Laboratory (NREL) for providing the equipment for our experiments.

Bashahu, M., & Nkundabakura, P. (2007). Review and tests of methods for the determination of the solar cell junction ideality factors. *Solar Energy*, *81*, 856–863.

Cameron, C. P., Boyson, W. E., & Riley, D. M. (2008). Comparison of pv system performance-model predictions with measured pv system performance. In *Photovoltaic Specialists Conference, 2008. PVSC '08. 33rd IEEE* (pp. 1 –6).

Campbell, R. C. (2007). A circuit-based photovoltaic array model for power system studies. *2007 39th North American Power Symposium*, (pp. 97–101).

Chan, D. S. H., & Phang, J. C. H. (1987). Analytical methods for the extraction of solar-cell single- and double-diode model parameters from i-v characteristics. *IEEE Transactions on Electron Devices*, *34*, 286–293.

Chenni, R., Makhlouf, M., Kerbache, T., & Bouzid, A. (2007). A detailed modeling method for photovoltaic cells. *Energy*, *32*, 1724–1730.

Davis, M. W., Dougherty, B. P., & Fanney, A. H. (2001). Prediction of building integrated photovoltaic cell temperatures. *Journal of Solar Energy Engineering*, *123*, 200–210.

Desoto, W., Klein, S., & Beckman, W. (2006). Improvement and validation of a model for photovoltaic array performance. *Solar Energy*, *80*, 78–88.

Duffie, J. A., & Beckman, W. A. (2006). *Solar Engineering of Thermal Processes*. New Jersey: John Wiley & Sons.

Jain, A., & Kapoor, A. (2004). Exact analytical solutions of the parameters of real solar cells using lambert w-function. *Solar Energy Materials and Solar Cells*, *81*, 269–277.

Jain, A., & Kapoor, A. (2005). A new method to determine the diode ideality factor of real solar cell using lambert w-function. *Solar Energy Materials and Solar Cells*, *85*, 391–396.

Khezzar, R., Zereg, M., & Khezzar, A. (2009). Comparative study of mathematical methods for parameters calculation of current-voltage characteristic of photovoltaic module. In *International Conference on Electrical and Electronics Engineering, 2009. ELECO 2009* (pp. I–24 – I–28).

Kim, S. K., JEON, J. H., CHO, C. H., KIM, E. S., & AHN, J. B. (2009). Modeling and simulation of a grid-connected pv generation system for electromagnetic transient analysis. *Solar Energy*, *83*, 664–678.

King, D. L. (1997). Photovoltaic module and array performance characterization methods for all system operating conditions. *Aip Conference Proceedings*, *394*, 347–368.

King, D. L., Boyson, W. E., & Kratochvil, J. A. (2004). Photovoltaic array performance model. *System*, (p. 39).

Masters, G. M. (2004). *Renewable and Efficient Electric Power Systems*. New Jersey: John Wiley & Sons.

Rajapakse, A. D., & Muthumuni, D. (2009). Simulation tools for photovoltaic system grid integration studies. In *Electrical Power Energy Conference (EPEC), 2009 IEEE* (pp. 1 –5).

Velasco-Quesada, G., Guinjoan-Gispert, F., Pique-Lopez, R., Roman-Lumbreras, M., & Conesa-Roca, A. (2009). Electrical pv array reconfiguration strategy for energy extraction improvement in grid-connected pv systems. *Industrial Electronics, IEEE Transactions on*, *56*, 4319 –4331.

Zhou, W., Yang, H., & Fang, Z. (2007). A novel model for photovoltaic array performance prediction. *Applied Energy*, *84*, 1187–1198.